Asian Journal of Chemistry; Vol. 36, No. 8 (2024), 1903-1911

ASIAN JOURNAL OF CHEMISTRY

https://doi.org/10.14233/ajchem.2024.31671

Multi Receptor Targeting of Potential Bioactive Compound Obtained from Chloroform Extract of *Asparagus racemosus* by GC-MS Analysis: A *in silico* Based Approach

SHAIK HARUN RASHEED, SAYYAD MUSTAK, CHANDAN MOHANTY, RAVI KUMAR VAKKALAGADDA and SANDIP SEN*

Department of Pharmaceutical Chemistry, School of Pharmacy, Guru Nanak Institutions Technical Campus, Ibrahimpatnam-501506, India

*Corresponding author: E-mail: sandipsen2010@gmail.com

Received: 6 April 2024; *Accepted*: 1 July 2024; *Published online*: 25 July 2024; AJC-21712

Previous reports indicate that the medicinal plants and their components have been utilized for treating diverse conditions since antiquity. *Asparagus racemosus*, in particular, demonstrates a broad spectrum of therapeutic possibilities. This study aimed to underscores the potential bioactive compounds found within the chloroform extract of *Asparagus racemosus*. Gas-chromatography employed to identify the presence of various molecules, while mass spectrometry and FTIR analysis validated their molecular structures. The molecules were analyzed to assess its suitability as a therapeutic candidate, their biological activity and predicted targets using *in silico* techniques. The chloroform extract stands out as the richest reservoir of carbohydrates and steroidal alkaloids. Molecule (5β)-pregnane-3,20β-diol, 14α,18α-[4-methyl-3-oxo-(1-oxa-4-azabutane-1,4-diyl)]diacetate was found in the highest concentration (42.28 %). The identified molecule is a steroidal alkaloid in nature and the computational analysis revealed promising drug-like properties and therapeutic potential for the investigated molecule.

Keywords: *Asparagus racemosus*, Chloroform, Gas chromatography, Mass spectroscopy, Drug likeliness, Target prediction.

INTRODUCTION

Many individuals exhibit reluctance towards the abundant synthetic and chemical medications available today, primarily due to their perceived adverse effects [1]. As a result, traditional herbal treatments are gaining traction in popularity, largely due to their perceived lack of adverse side effects and minimal ecological footprint [2]. Although there are many effective modern synthetic medications available, more and more individuals are choosing plant-based natural remedies [3]. This inclination arises from the diverse phytoconstituents present in various plant parts, which can treat and cure diseases [3-5]. The practice of using plants as medicine is deeply rooted in the Indian medical tradition, with evidence indicating its prevalence since ancient times [6].

Medicinal plants provide more than a quarter of the active ingredients present in modern prescription medications [7]. Bioactive chemicals isolated from these plants are associated with a range of pharmacological actions, including antioxidant, anticancer, antifungal, anti-inflammatory and antibacterial properties [8]. Therefore, it is crucial to evaluate the potential of these bioactive compounds to comprehend their viability in treating different ailments [9]. The basis of many highly efficient medications originates from the bioactive compounds extracted and identified from the medicinal plants [10]. Understanding the chemical and pharmacological actions of these herbs relies heavily on chromatographic and spectrophotometric techniques [11,12]. The utilization of the GC-MS approach considered a proper procedure, allows for the detection of various bioactive compounds [13].

Plants categorized under the genus *Asparagus racemosus*, commonly known as Salwar, Satamuli and Satavari, are native to low-altitude regions in India and are part of the Liliaceae family [14] and the dried roots of this plant are utilized in medicines. The roots are attributed with ulcer-healing properties, likely achieved by enhancing mucosal resistance or providing cytoprotection [15]. Additionally, recent studies indicate its effectiveness in reducing AIDS symptoms, as well as its historical use by Ayurvedic practitioners for treating neurological issues [16]. The root extract of *A. racemosus* has been utilized for diverse applications, there is a scarcity of scientific evidence substantiating these assertions. Nonetheless, some research

suggests the beneficial effects of *A. racemosus* root extracts, including galactagogue properties, antihepatotoxic effects, immunomodulatory effects, immunoadjuvant effects, antilithiatic effects and teratogenicity [16].

In recent times, the development of new drugs has increasingly leaned on computer-aided technologies. Identifying active molecules from phytochemicals in medicinal plants has become more streamlined [17]. In recent times, the development of new drugs has increasingly leaned on computer-aided technologies [18]. Techniques utilizing non-covalent ligand binding are notably advantageous in systems biology, facilitating precise ligand binding to the active sites of target macromolecules [19]. The chloroform extract derived from *A. racemosus* underwent GC-MS analysis to identify its bioactive constituents. Following this, potential bioactive compounds were further examined utilizing the computer-aided molecular analysis and *in silico* methodologies.

EXPERIMENTAL

Fresh stems of shatavari (*Asparagus racemosus*) were collected from Ibrahimpatnam, Rangareddy District, India, situated at an altitude of 373 meters at coordinates 16.5811ºN 77.7489ºE. Authentication of the plant materials was conducted by the Department of Botany, Osmania University, Hyderabad, India.

Preparation of extracts: The fresh plant materials were subjected to air-drying under shaded conditions at 40 ± 5 ºC. After drying, the plant material was ground into a coarse powder using a Crompton TRET500 mixer and grinder, manufactured in India. The powdered material was then moistened with chloroform and subjected to extraction using a Soxhlet apparatus. About 200 g of stem powder was placed inside a muslin cloth bag with a mesh size of 100. The stem powder was defatted with petroleum ether. The extraction process utilized 1 L chloroform and proceeded until a colourless liquid was achieved. The chloroform layer was subsequently gathered employing a rotary flash evaporator under reduced pressure conditions at 55 ºC and 50 rpm (Aditya Scientific RE-2A rotary evaporator, Hyderabad, India). The residue obtained was dried completely in a desiccator and the percentage yield was calculated [20].

Phytochemical analysis: The petroleum ether extract was subjected to phytochemical testing by literature procedure [21].

GC-MS analysis: The GC-MS analysis was performed using the Agilent 7890A GC System coupled with the AccuTOF GCv/JMS-T100GCv from JEOL. For the analysis, 25 mg of chloroform extract was weighed and dissolved in 100 mL of methanol of HPLC-grade quality. The resulting mixture was further diluted to a concentration of 30 µg/mL. The total runtime for the scanning was 50 min. The sample was injected into an HP5 Column with dimensions of 30 m × 0.25 mm × 0.25 µ, and the carrier gas helium was supplied at a flow rate of 1 mL/min. The oven temperature was maintained at 280 ºC. The compounds isolated during the analysis were identified by comparing their mass spectra with NIST library database [21].

Preparation of structure: The SMILES notation of the compounds generated using ACD labs Chemsketch version 12.0, Bangalore, India.

Calculation of molecular and physico-chemical properties and toxicity potential of compounds: The molecular and physico-chemical properties, along with the toxicity potential, were determined using the Osiris Data Warrior software and the Swiss ADME online tool. Additionally, the absorption percentage (%Abs) was calculated using the following eqn:

$$Abs\ (\%) = 109 - (0.345 \times TPSA)$$

Calculation of drug likeliness, bioactivity score and pharmacokinetic potential: The drug likeliness and toxicity potential were predicted using Swiss ADME (http://www.swissadme.ch/index.php). The Bioavailability score against various types of receptors was determined using Molinspiration software version 2011.06. A bioactivity radar of molecules was generated using the Swiss ADME tool [22].

Calculation of pharmacokinetic potential: The pharmacokinetic properties related to absorption, permeation, excretion and metabolism including CYP1A2 inhibitor, CYP2C19 inhibitor, CYP2C9 inhibitor, CYP2D6 inhibitor, CYP3A4 inhibitor and log Kp (skin permeation) were computed using Swiss ADME. Additionally, the Swiss ADME tool produced the boiled egg diagram [22].

Target prediction: The therapeutic effectiveness of the identified molecule was predicted using Swiss target prediction. The SMILES notation of the molecule was entered into an online tool to forecast its target. The obtained results included target, target class and probability, which were used to interpret the findings. The target with the highest probability was regarded as significant for the molecule under scrutiny. This procedure provided valuable insights into the identification of particular proteins and the therapeutic possibilities of the drug [23].

RESULTS AND DISCUSSION

This work was intended to identify a number of non-polar biomolecules present in an *Asparagus racemosus* chloroform extract. The chromatographic analysis was used to identify the various types of molecules present in extract, whereas the spectral analysis confirmed the structures of the identified compounds. The drug-like behavior of the various components in the extract was validated by *in silico* and target prediction. This study focused on assessing the target potential of the plant extract, aiming to discern its molecular identity for desired therapeutic potential.

Phytochemical analysis: The chloroform extract exhibited a yield of 14.8% and the subsequent analysis unveiled the existence of alkaloids, flavonoids, steroids, phenolic compounds, terpenoids and aliphatic compounds within the extract.

GC-MS studies: The maximum percentage peak areas 13.54, 19.37 and 42.28 % were observed for the molecules **2**, **7** and **8**. The retention time was found to be 7.03, 19.59 and 23.44, respectively for the respective compounds (Fig. 1 and Table-1). The structure of the compounds was confirmed by mass spectroscopy (Fig. 2) and eleven compounds were identified in the chloroform extract (Fig. 3).

FTIR studies: Functional groups within various molecules were confirmed in the chloroform extract of *A. racemosus* using the FTIR spectrum. The FTIR peaks at 3371 cm^{-1} (-NH-,

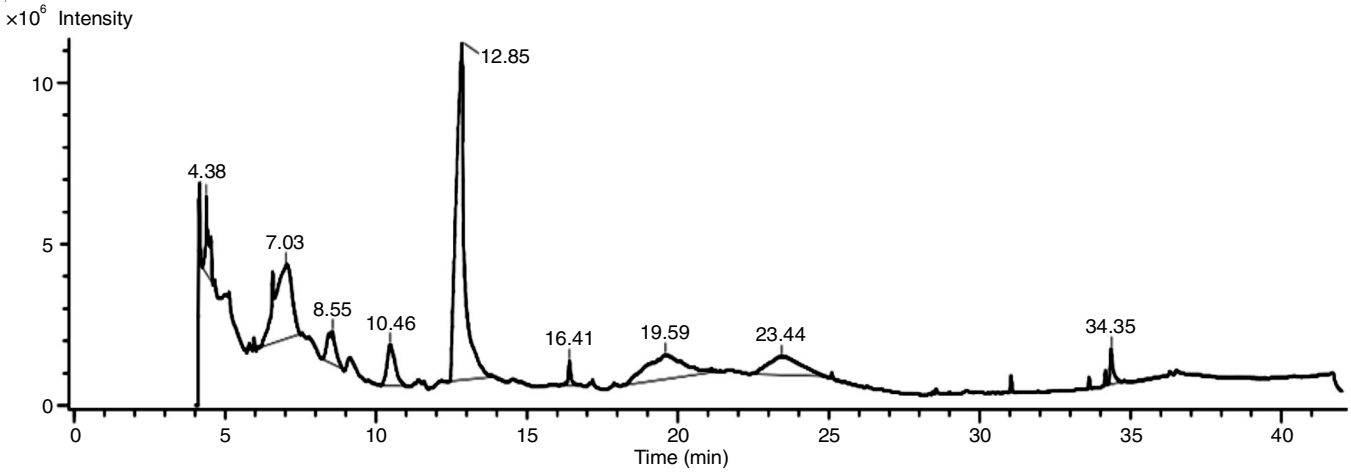

Fig. 1. Chromatographic profile of the chloroform extract of *Asparagus racemosus* obtained *via* GC

TABLE-1
GAS CHROMATOGRAPHY ANALYSIS OF CHLOROFORM EXTRACT OF *Asparagus racemosus* (SHATAVARI)

Peak number	Time (min)	Area (intens. * sec)	Peak area (%)	Height	m.w.	m.f.
1	4.38	18827666.53	3.87	2403869	118	$C_2H_6N_4O_2$
2	7.03	65842602.32	13.54	756266	504	$C_{18}H_{32}O_{16}$
3	8.55	19143336.55	3.93	1011222	128	$C_6H_8O_3$
4	10.46	23770657.63	4.89	1273581	144	$C_6H_8O_4$
5	12.85	42855268.47	8.81	560946	489	$C_{28}H_{43}NO_6$
6	16.41	5064551.22	1.04	745679	261	$C_{16}H_{36}FN$
7	19.59	94167336.59	19.37	2309504	180	$C_6H_{12}O_6$
8/5	23.44	205528605.7	42.28	104552057	126	$C_6H_6O_3$
9	33.62	1060775.73	0.21	346798	446	$C_{25}H_{34}O_7$
10	34.16	1781217.83	0.36	467654	1058	$C_{16}H_{134}O_6$
11	34.35	8054467.31	1.65	1109073	568	$C_{35}H_{68}O_5$

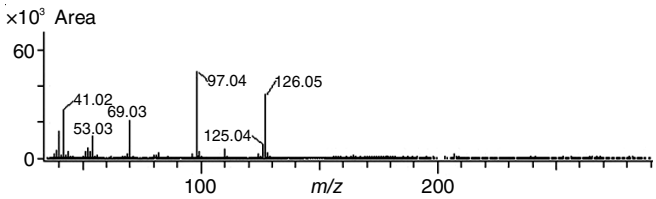

Fig. 2. Mass spectrum of molecule-8 identified in the chloroform extract of *Asparagus racemosus*

str.); 3295 cm^{-1}(OH *str.*); 3174 cm^{-1} (OH *str.*, -COOH); 2810 cm^{-1} (C=N *str.*); 2685 cm^{-1} (C=O *str.*, -COOH); 1627.70 cm^{-1} (C=O *str.*); and 1414.61 cm^{-1} (N-CH_3 *str.*) indicated the presence of molecule **8** (Fig. 4).

Molecular property: Factors such as molecular shape, flexibility and complexity significantly impact the effectiveness of drug action and receptor binding. Generally, molecules with a spherical shape are thought to demonstrate improved absorption [24]. Additionally, increased flexibility and reduced molecular complexity are typically advantageous for efficient receptor binding [25,26]. These findings are summarized in Table-2. Specifically, molecules **7**, **8** and **9** exhibit the spherical shapes remaining molecules demonstrate linear shapes, while molecules **2**, **6** and **7** display high flexibility. Additionally, all the molecules exhibit increased molecular complexity except molecule **6**.

TABLE-2
MOLECULAR PROPERTIES OF THE MOLECULES IDENTIFIED BY GC-MS ANALYSIS

Molecule	Index	Flexibility	Complexity
1	0.75	0.46	0.69
2	0.83	0.75	0.80
3	0.55	0	0.84
4	0.60	0.30	0.75
5	0.77	0.39	0.74
6	0.52	0.67	0.35
7	0.41	0.59	0.93
8	0.45	0.39	0.96
9	0.43	0.22	1.02
10	0.65	0.56	0.65
11	0.90	0.57	0.58

a: Molecular shape index (spherical: ≤ 0.5, linear: ≥ 0.5); b: Molecular flexibility (low: ≤ 0.5, high: ≥ 0.5); c: molecular complexity (low: ≤ 0.5, high: ≥ 0.5).

Physico-chemical properties: The physico-chemical properties of molecules significantly influence their biological activity and drug likeliness [27,28] and the results are summarized in Table-3 and Fig. 5. Molecules **3**, **4**, **6**, **8** and **9** exhibit cLogP values of 0.06-3.28. For molecules **10** and **11**, the value 27.24 and 12.24 indicate high toxicity, however, except for molecules **2**, **3**, **4**, **5** and **6**, all molecules possess more than 5 hydrogen acceptor sites. Additionally, all molecules have fewer

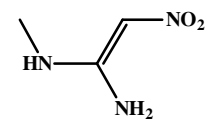

Molecule 1:
N-methyl-N'-niroguanidine

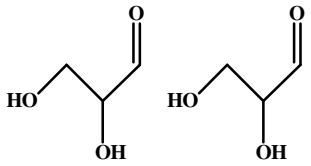

Molecule 2:
Diglyceraldehyde dimer

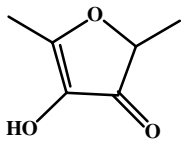

Molecule-3:
4-Hydroxy-2,5-dimethylfuran-3(2*H*)-one

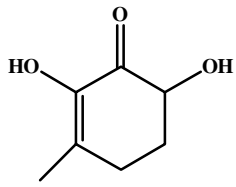

Molecule 4:
2,6-Dihydroxy-3-methylcyclohex-2-enone

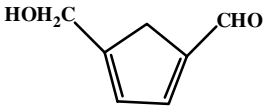

Molecule 5:
4-(Hydroxymethyl)cyclopenta-1,3-dienecarbaldehyde

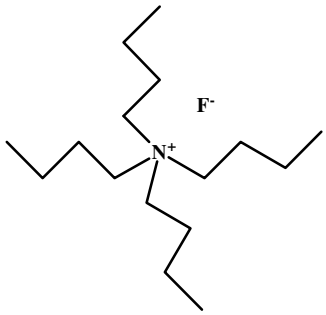

Molecule 6:
Tetrabutylammonium fluoride

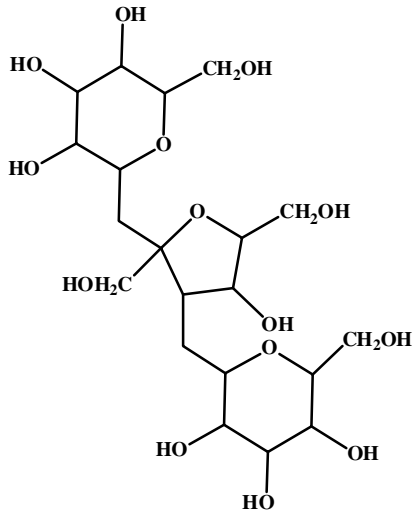

Molecule 7: Melezitose

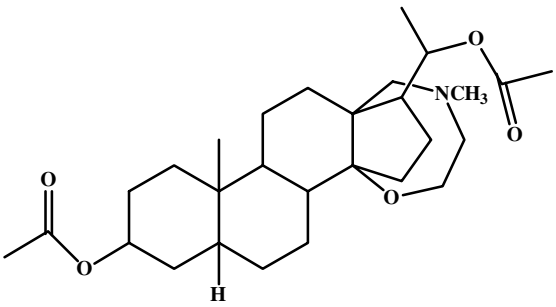

Molecule 8:
(5β)Pregnane-3,20β-diol,14α,18α-[4-methyl-3-oxo-(1-oxa-4-azabutane-1,4-diyl)]-, diacetate

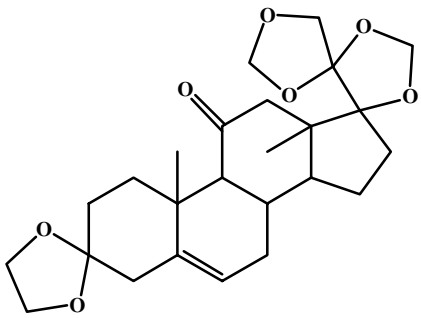

Molecule 9:
Pregn-5-ene-3,11-dione, 17,20:20,21-*bis*[methylene*bis*(oxy]]-, cyclic 3-(1,2-ethanediyl acetal)

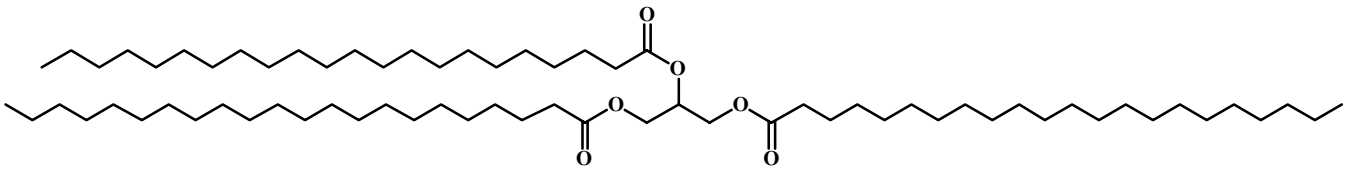

Molecule 10: Docosanoic acid, 1,2,3-propanetriyl ester

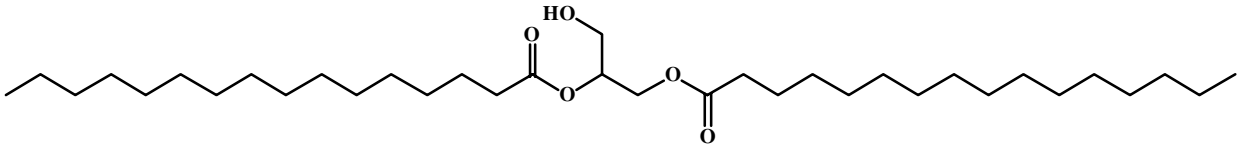

Molecule 11: 1,2,dipalmitin

Fig. 3. Molecular structures identified in the chloroform extract of *Asparagus racemosus*

TABLE-3
PHYSICAL AND CHEMICAL TRAITS OF THE MOLECULES DETECTED *via* GC ANALYSIS

Molecule	cLogP	cLogS	H-acceptors	H-donors	Total surface area	Relative PSA	MR	TPSA	% Abs	Solubility
1	-2.1627	-2.132	5	2	94.12	0.6072	29.68	83.87	80.06	Very soluble
2	-1.6559	-0.056	3	2	72.00	0.545	38.12	115.06	69.30	Highly soluble
3	0.0641	-1.432	3	1	94.04	0.3843	31.22	46.53	92.94	Very soluble
4	0.1565	-1.23	3	2	105.65	0.37142	36.11	57.53	89.15	Very soluble
5	-0.0261	-0.873	2	1	102.83	0.25421	34.06	37.3	96.13	Very soluble
6	2.187	-2.902	1	0	233.54	-0.032628	82.51	0	109	Very soluble
7	-5.8796	0.199	14	11	328.32	0.53028	107.98	250.22	22.67	Highly soluble
8	3.281	-4.453	7	0	358.44	0.20274	136.32	82.14	80.66	Moderately soluble
9	2.2898	-4.765	7	0	300.65	0.24294	113.32	72.45	84.00	Soluble
10	27.274	-17.271	6	0	999.15	0.069179	337.65	78.9	81.77	Insoluble
11	12.249	-8.221	5	1	525.17	0.11269	174.09	72.83	83.87	Poorly soluble

a: Partition coefficient (P = [*n*-octanol]/[water]) (cLogP); b: Solubility in water (S = mol/L at pH = 7.5, 25 °C) (cLogS); c: Relative polar surface area (relative PSA); d: Molar refractive index; e: Topological polar surface area (TPSA); f: Absorption percentage (%Abs).

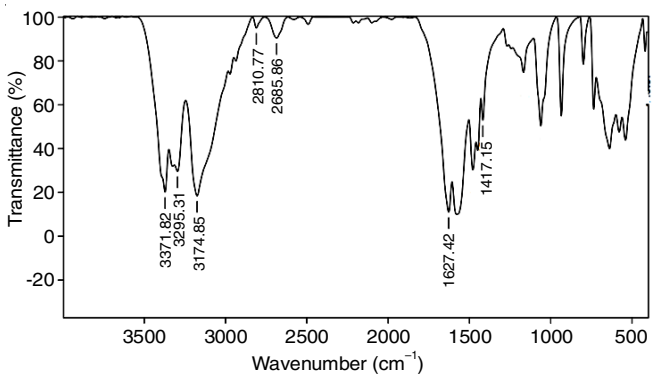

Fig. 4. FTIR of molecule-8 identified in the chloroform extract *Asparagus racemosus*

than 10 hydrogen donor sites except molecule **7**. Moreover, molecules **6**, **7** and **9** have a molar refractive index ranging from 40 to 130. Similarly, total polar surface area (TPSA) values fall within the range of 90-140 for all molecules except molecules **6** and **7**.

Drug likeness: Identified molecules followed the Lipinski rule except for molecules **7**, **10** and **11**. Only molecules **6** and **10** followed the Ghose rule. Similarly, except the molecules **6**, **7**, **10** and **11** other molecules followed Veber and Egan rules. Similarly, no molecules except **8** and **9** followed the Muegge rules. From the thorough analysis, it was found that molecules **7**, **10** and **11** do not follow drug-likeliness behaviour [29]. The bioavailability score was determined to be 0.55 for all molecules except **7**, **10** and **11** (0.17). Furthermore, molecules **4** and **8** exhibited positive drug-likeness values of 0.42 and 2.82, respectively. These findings indicate that molecule **8** possesses favorable drug-like properties (Table-4).

Bioactivity score and toxicity profiles: The hierarchy of bioactivity for molecules with target receptors is as follows: EI > IC > GL > PI > NR > KI, as depicted in Table-5. Molecule **8** exhibited bioactivity scores greater than zero with various receptors and displayed a significant binding affinity for multiple receptors [30]. Molecule **2** exhibited high mutagenic properties, whereas molecule **5** was found to possess irritant characteristics (Table-6).

Pharmacokinetics profiles: The absorption of the active molecule occurs primarily through a diffusion process. When considering bimolecular substances, GI absorptivity and human intestinal absorption (HIA) are the crucial parameters [31,32]. The small intestine offers a greater area for drug absorption

TABLE-4
DRUGLIKLINESS OF THE MOLECULES IDENTIFIED BY GC-MS ANALYSIS

Molecule	Drug likeness	Lipinski	Ghose	Veber	Egan	Muegge	Bioavailability score
1	-5.0285	0	GR4	0	0	MR2	0.55
2	-3.7931	0	GR2	0	0	MR2	0.55
3	-0.88539	0	GR2	0	0	MR1	0.55
4	0.42243	0	GR2	0	0	MR1	0.55
5	-6.8875	0	GR3	0	0	MR1	0.55
6	-4.9863	0	0	VR1	0	MR1	0.55
7	-6.1645	LR3	GR2	VR1	ER1	MR4	0.17
8	2.8223	0	GR3	0	0	0	0.55
9	-5.6255	0	0	0	0	0	0.55
10	-26.013	LR2	GR4	VR1	ER1	MR3	0.17
11	-26.084	LR2	GR4	VR1	ER1	MR2	0.17

LR2: violations: MW > 500, MLOGP > 4.15, LR3: violations: MW > 500, NorO > 10, NHorOH > 5, GR2: violations: MW > 480, WLOGP < -0.4, GR3: violations: MW > 480, MR > 130, #atoms > 70, GR4: violations: MW > 480, WLOGP > 5.6, MR > 130, #atoms > 70, VR1: violation: Rotors > 10 and TPSA > 140, ER1: violation: TPSA > 131.6 and violation: WLOGP > 5.88, MR1: violation: Heteroatoms < 2, MR2: violations: XLOGP3 > 5, Rotors > 15, MR3: No; 3 violations: MW > 600, XLOGP3 > 5, Rotors > 15, MR4: violations: XLOGP3 < -2, TPSA > 150, H-acc > 10, H-don > 5.

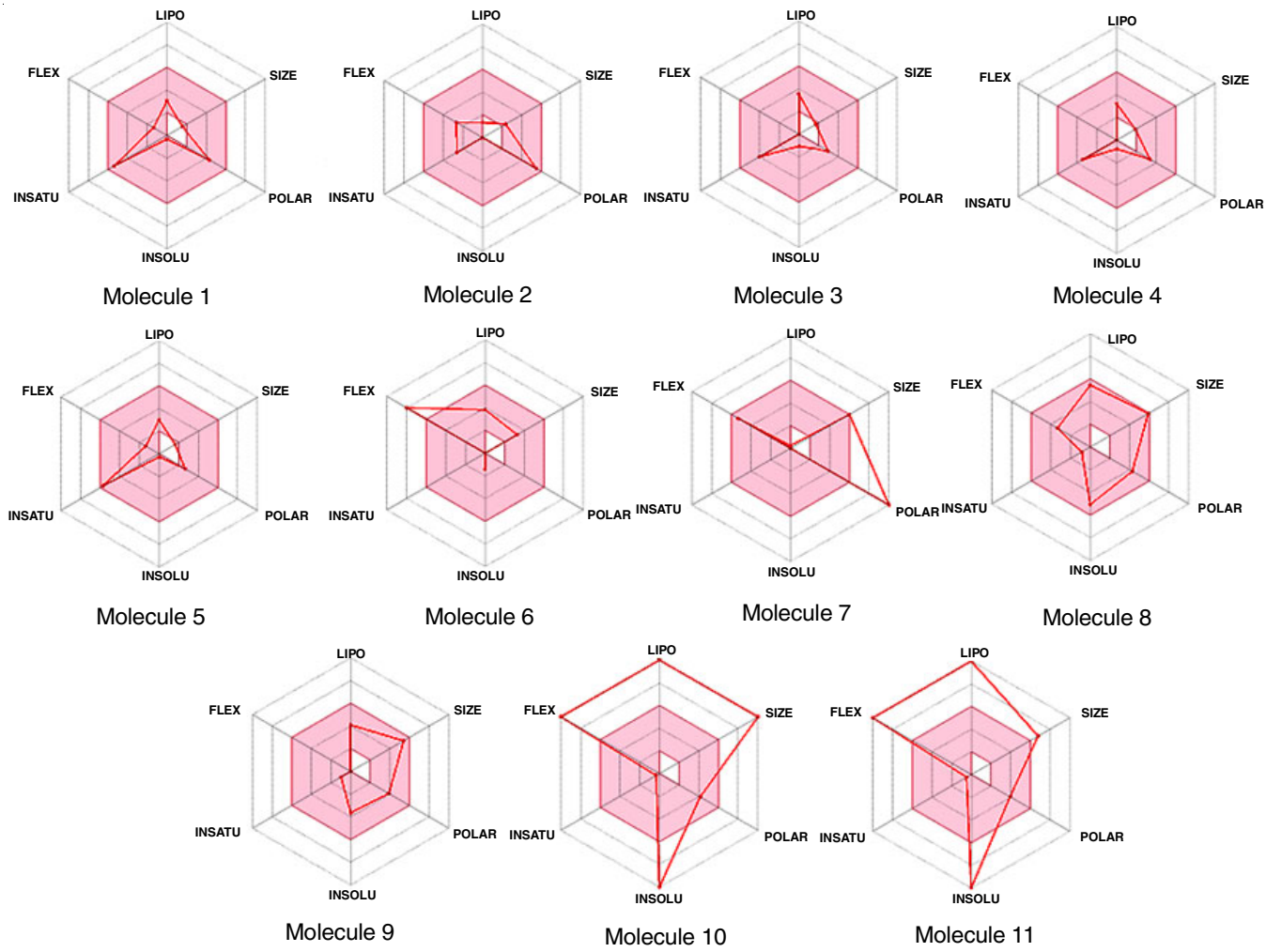

Fig. 5. Bioactivity rader for molecules in chloroform extract of *Asparagus racemosus*

TABLE-5
BIOACTIVITY SCORES FOR THE MOLECULES PINPOINTED *via* GC-MS ANALYSIS

Molecule	GL	IC	KI	NR	PI	EI
1	-3.24	-2.8	-3.42	-3.77	-2.96	-2.44
2	-3.59	-3.53	-3.66	-3.49	-3.03	-2.8
3	-2.73	-1.8	-3.43	-2.57	-2.78	-1.61
4	-1.17	-0.46	-1.85	-0.63	-1.1	0.03
5	-1.9	-1.43	-2.1	-1.7	-1.9	-0.99
6	0.03	0.28	-0.49	-0.82	-0.54	0.2
7	0.1	0.1	-0.38	0.35	0.09	0.23
8	0.22	0.16	0.1	0.12	0.22	0.41
9	0.01	0.04	-0.54	0.38	-0.15	0.53
10	-3.72	-3.81	-3.8	-3.81	-3.65	-3.75
11	0.1	-0.25	-0.07	-0.04	0.08	0.08

≥ 0: Good, 0-0.5: Moderate, ≤ 0.5: Poor; GL: GPCR ligand, IC: Ion channel modulator, KI: Kinase inhibitor, NR: Nuclear receptor ligand, PI: Protease inhibitor, EI: Enzyme inhibitor.

TABLE-6
ASSESSMENT OF THE TOXICITY POTENTIAL LINKED TO THE MOLECULES IDENTIFIED THROUGH GC-MS ANALYSIS

Molecule	Mutagenic	Tumorigenic	Reproductive effective	Irritant
1	–	–	–	–
2	++	–	–	–
3	–	–	–	–
4	–	–	–	–
5	–	–	–	++
6	–	–	–	–
7	–	–	–	–
8	–	–	–	–
9	–	–	+	–
10	–	–	–	–
11	–	–	–	–

than the stomach does. Furthermore, the blood-brain barrier controls the passage of drug molecules into the central nervous system, thus averting cytotoxic effects [33].

P-glycoprotein (PGP) is pivotal in the process of drug excretion and distribution [34]. It acts as a deterrent to drug absorption in both oral bioavailability and the blood-brain barrier, curtailing drug buildup in the brain. Inhibiting PGP can result in drug interactions and heightened drug accumulation in brain [35]. Cytochrome P450 (CYP) enzymes are vital for drug metabolism. If certain drugs inhibit these enzymes, it can decrease drug metabolism and other metabolic activities. GI absorptivity is high for molecules **2**, **6**, **7**, **10** and **11** and blood-brain barrier (BBB) penetrability was observed for molecules **3**, **5** and **9**. Higher human intestinal absorption (HIA)

capacity was observed for molecules **1**, **4**, **5**, **8** and **9**. Molecules **6**, **7** and **10** exhibited the PGP efflux effect, whereas none of them showed any CYP inhibitory effect. The findings indicate that the skin permeability of the molecules is within an acceptable range (Table-7 and Fig. 6).

Prediction and analysis of molecular targets: Based on the bioactivity score, target prediction analysis was conducted for all the molecules with the results presented in Table-8 and correlated with the results obtained during GC-MS and *in silico* studies. The analysis revealed that molecule **8** targets the G-Protein coupled Kappa Opioid receptor, suggesting its potential use as an anti-inflammatory analgesic, diuretic and antistress antiepileptic drug. It also exhibits binding affinity with electrochemical transporters, specifically Glycine transporter 1 and 2, crucially regulating glycine levels at inhibitory synapses solely during early postnatal life. Additionally, it governs the dynamics of synaptic vesicle refilling in inhibitory spinal cord neurons. As a thymidine kinase enzyme inhibitor, it acts as a potent anticancer drug. It is also important in the detoxification of genotoxic compounds by binding with protease epoxide hydratase.

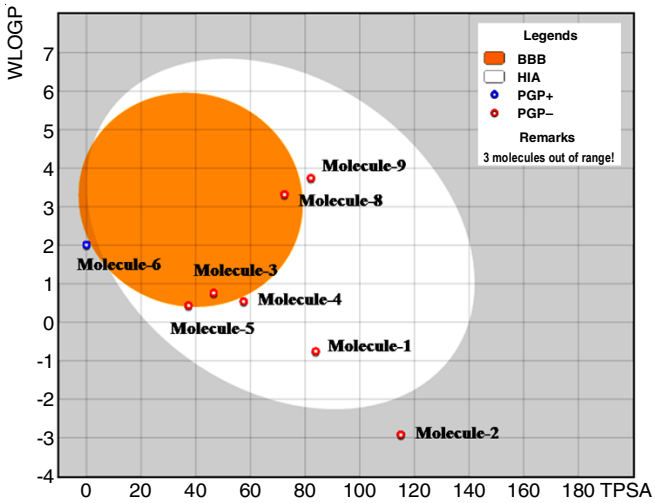

Fig. 6. Schematic representation of molecules identified in the chloroform extract of *A. racemosus*, akin to a BOILED EGG diagram

Thus, molecule **8** can be a significant biomolecule isolated from *A. racemosus* for the treatment of multiple disorders [36].

TABLE-7
PHARMACOKINETIC CAPABILITIES OF THE MOLECULES PINPOINTED THROUGH GC-MS ANALYSIS

Molecule	GI absorption	BBB permeant	Pgp substrate	CYP1A2 inhibitor	CYP2C19 inhibitor	CYP2C9 inhibitor	CYP2D6 inhibitor	CYP3A4 inhibitor	log Kp (cm/s)
1	++	–	–	–	–	–	–	–	-7.12
2	+	–	–	–	–	–	–	–	-9.64
3	++	Y	–	–	–	–	–	–	-6.60
4	++	–	–	–	–	–	–	–	-7.09
5	++	Y	–	–	–	–	–	–	-7.26
6	+	–	Y	–	–	–	–	–	-7.04
7	+	–	Y	–	–	–	–	–	-12.99
8	++	–	–	–	–	–	–	–	-6.43
9	++	Y	–	–	–	–	–	–	-7.86
10	+	–	Y	–	–	–	–	–	9.74
11	+	–	Y	–	–	–	–	–	0.20

TABLE-8
PREDICTING TARGETS FOR THE MOLECULES, DETAILING THEIR BIOLOGICAL ROLES AND THERAPEUTIC IMPLICATIONS

Molecule	Target	Target Class	Probability*	Functions
1	Toll-like receptor (TLR7/TLR9)	Toll-like and Il-1 receptors	0.03	Antiviral immune responses
2	Aldose reductase	Enzyme	0.99	Antidiabetic
3	Carbonic anhydrase II	Lyase	0	Analgesic and anticancer
4	Cytochrome P450 19A1	Cytochrome P450	0.05	Hormonal supplement for female sex hormones
	Corticosteroid binding globulin	Secreted protein	0.05	It facilitates the transportation of glucocorticoids and progesterone in the bloodstream, thereby regulating the tissue availability of these hormones.
	Testis-specific androgen-binding protein	Secreted protein	0.05	Spermatogenesis and epididymal sperm maturation
	Carboxylesterase 2	Enzyme	0.05	Anticancer
5	γ-Butyrobetaine dioxygenase	Enzyme	0.02	Inhibition of L-carnitine biosynthesis pathway.
	PI3-kinase p110α/p85α	Enzyme	0.02	Anticancer and antiplatelet drugs
6	Target not identified			
7	β-Glucocerebrosidase	Enzyme	0.12	Antidiabetic
	Pancreatic α-amylase	Hydrolase	0.12	Antidiabetic
	Sucrase-isomaltase	Enzyme	0.12	Antidiabetic
	P-glycoprotein 1	Primary active transporter	0.12	Preserving the integrity of the blood-brain barrier and facilitating the removal of drugs from the kidneys into urine and from the liver into bile.
	Glutamate carboxypeptidase II	Protease	0.12	Therapy for prostate cancer (PCa).

8	κ-Opioid receptor	Family A G protein-coupled receptor	0.11	It serves essential functions in pain modulation, diuresis, stress response, reward processing, mood regulation, cognitive function, management of epileptic seizures, and perception of itchiness.
	Glycine transporter 1	Electrochemical transporter	0.11	Critical for regulating glycine levels at inhibitory synapses during early postnatal development.
	Glycine transporter 2	Electrochemical transporter	0.11	GlyT2 governs synaptic vesicle refilling in inhibitory spinal cord neurons.
	Thymidine kinase, mitochondrial	Enzyme	0.11	Anticancer
	Epoxide hydratase	Protease	0.11	Essential for detoxifying genotoxic compounds and regulating physiological signals.
9	Target not identified			
10	Protein kinase C γ (by homology)	Kinase	0.25	Anticancer
	Protein kinase C α	Kinase	0.25	Anticancer
	Protein kinase C epsilon	Kinase	0.25	Anticancer and antidiabetic
11	Protein kinase C θ	Kinase	0.69	It represents an attractive drug target for allergic and autoimmune diseases.

Conclusion

This study identified 7 molecules from the chloroform extract of *Asparagus racemosus* through gas chromatographic analysis, with their structures confirmed *via* mass spectroscopy and FTIR studies. Among them, the highest concentration was observed for (5β)-pregnane-3,20β-diol, 14α,18α-[4-methyl-3-oxo-(1-oxa-4-azabutane-1,4-diyl)]diacetate. Among the identified molecules, molecule-**8** exhibits the spherical shapes and good to moderate molecular flexibility, displaying favourable drug-likeliness characteristics without any observed toxicity. Moreover, molecule-**8** also demonstrates higher human intestinal absorption (HIA) capacity. Target prediction analysis identifies molecule-**8** as a potential therapeutic molecule, suggesting its efficacy as an analgesic, anti-inflammatory, anti-epileptic, diuretic and neoplastic agent.

ACKNOWLEDGEMENTS

The authors acknowledge their sincere thanks to SAIF, IIT Bombay for GC-MS and FTIR analyses. Thanks are also due tothe School of Pharmacy, Guru Nanak Institutions Technical Campus for providing all the facilities for the study.

CONFLICT OF INTEREST

The authors declare that there is no conflict of interests regarding the publication of this article.

REFERENCES

1. D. Galeano, S. Li, M. Gerstein and A. Paccanaro, *Nat. Commun.*, **11**, 4575 (2020); https://doi.org/10.1038/s41467-020-18305-y
2. N. Sahoo and P. Manchikanti, *J. Altern. Complement. Med.*, **19**, 957 (2013); https://doi.org/10.1089/acm.2012.0275
3. H. Yuan, Q. Ma, L. Ye and G. Piao, *Molecules*, **21**, 559 (2009); https://doi.org/10.3390/molecules21050559
4. U. Anand, N. Jacobo-Herrera, A. Altemimi and N. Lakhssassi, *Metabolites*, **9**, 258 (2019); https://doi.org/10.3390/metabo9110258
5. D.K. Semwal, A. Chauhan, A. Kumar, S. Aswal, R.B. Semwal and A. Kumar, *J. Integr. Med.*, **17**, 238 (2019); https://doi.org/10.1016/j.joim.2019.04.008
6. M.M. Pandey, S. Rastogi and A.K.S. Rawat, *Evid. Based Complement. Alternat. Med.*, **2013**, 376327 (2013); https://doi.org/10.1155/2013/376327
7. F. Malongane, L.J. McGaw and F.N. Mudau, *J. Sci. Food Agric.*, **97**, 4679 (2017); https://doi.org/10.1002/jsfa.8472
8. R. Yadav, R.K. Khare and A. Singhal, *Int. J. Life. Sci. Sci. Res.*, **3**, 844 (2017).
9. A.M. Juszczak, M. Zovko-Konèic and M. Tomczyk, *Biomolecules*, **9**, 731 (2019); https://doi.org/10.3390/biom9110731
10. P. Satapute, M.K. Paidi, M. Kurjogi and S. Jogaiah, *Environ. Pollut.*, **251**, 555 (2019); https://doi.org/10.1016/j.envpol.2019.05.054
11. S. Fan, J. Chang, Y. Zong, G. Hu and J. Jia, *Molecules*, **23**, 576 (2018); https://doi.org/10.3390/molecules23030576
12. S. Razack, K.H. Kumar, I. Nallamuthu, M. Naika and F. Khanum, *Antioxidants*, **4**, 185 (2015); https://doi.org/10.3390/antiox4010185
13. S. Mirunalini and M. Krishnaveni, *J. Basic Clin. Physiol. Pharmacol.*, **21**, 93 (2010); https://doi.org/10.1515/JBCPP.2010.21.1.93
14. R. Vishwakarma and P.K. Goswami, *Ayu*, **34**, 17 (2013); https://doi.org/10.4103/0974-8520.115438
15. J.P. Kamat, K.K. Boloor, T.P. Devasagayam and S.R. Venkatachalam, *J. Ethnopharmacol.*, **71**, 425 (2000); https://doi.org/10.1016/S0378-8741(00)00176-8
16. G. Sliwoski, S. Kothiwale, J. Meiler and E.W. Lowe Jr., *Pharmacol. Rev.*, **66**, 334 (2013); https://doi.org/10.1124/pr.112.007336
17. K. Lee and D. Kim, *Genes*, **10**, 906 (2019); https://doi.org/10.3390/genes10110906
18. I. Lamers and P. Feys, *Mult. Scler.*, **20**, 775 (2014); https://doi.org/10.1177/1352458514525677
19. D.S. Kumar, D. Karthikeyan and B. Roy, *Asian J. Chem.*, **34**, 342 (2022); https://doi.org/10.14233/ajchem.2022.23521
20. G.M. Morris and M. Lim-Wilby, *Methods Mol. Biol.*, **443**, 365 (2008); https://doi.org/10.1007/978-1-59745-177-2_19
21. B. Chibuye, I.S. Singh, L. Chimuka Luke and K.K. Maseka, *Sci. African*, **19**, e01585 (2023); https://doi.org/10.1016/j.sciaf.2023.e01585
22. S. Sen, B. Ravindar, S. Jala and L. Dharabonia, *Int. J. Pharm. Sci. Res.*, **13**, 3163 (2022); https://doi.org/10.13040/IJPSR.0975-8232.13(8).3163-73
23. D.S. Kumar, D. Karthikeyan and B. Roy, *Asian J. Chem.*, **34**, 1401 (2022); https://doi.org/10.14233/ajchem.2022.23624

24. A. Nicholls, G.B. McGaughey, R.P. Sheridan, A.C. Good, G. Warren, M. Mathieu, S.W. Muchmore, S.P. Brown, J.A. Grant, J.A. Haigh, N. Nevins, A.N. Jain and B. Kelley, *J. Med. Chem.*, **53**, 3862 (2010); https://doi.org/10.1021/jm900818s
25. R. Rohs, I. Bloch, H. Sklenar and Z. Shakked, *Nucleic Acids Res.*, **33**, 7048 (2005); https://doi.org/10.1093/nar/gki1008
26. O. Méndez-Lucio and J.L. Medina-Franco, *Drug Discov. Today*, **22**, 120 (2017); https://doi.org/10.1016/j.drudis.2016.08.009
27. L.Z. Benet, C.M. Hosey, O. Ursu and T.I. Oprea, *Adv. Drug Deliv. Rev.*, **101**, 89 (2016); https://doi.org/10.1016/j.addr.2016.05.007
28. S. Prasanna and R.J. Doerksen, *Curr. Med. Chem.*, **16**, 21 (2009); https://doi.org/10.2174/092986709787002817
29. D. Ji, M. Xu, C.C. Udenigwe and D. Agyei, *Curr. Res. Food Sci.*, **3**, 41 (2020); https://doi.org/10.1016/j.crfs.2020.03.001
30. A. Husain, A. Ahmad, S.A. Khan, M. Asif, R. Bhutani and F.A. Al-Abbasi, *Saudi Pharm. J.*, **24**, 104 (2016); https://doi.org/10.1016/j.jsps.2015.02.008
31. L.F. Prescott, *Med. Clin. North Am.*, **58**, 907 (1974); https://doi.org/10.1016/S0025-7125(16)32088-0
32. M.D. Wessel, P.C. Jurs, J.W. Tolan and S.M. Muskal, *J. Chem. Inf. Comput. Sci.*, **38**, 726 (1998); https://doi.org/10.1021/ci980029a
33. W.M. Pardridge, *J. Cereb. Blood Flow Metab.*, **32**, 1959 (2012); https://doi.org/10.1038/jcbfm.2012.126
34. Y. Tanigawara, *Ther. Drug Monit.*, **22**, 137 (2000); https://doi.org/10.1097/00007691-200002000-00029
35. J.H. Lin and A.Y. Lu, *Clin. Pharmacokinet.*, **35**, 361 (1998); https://doi.org/10.2165/00003088-199835050-00003
36. D Gfeller, A Grosdidier, M Wirth, A Daina, O Michielin, V Zoete, *Nucleic Acids Res.*, **42(Web Server issue)**, W32-8 (2014); https://doi.org/10.1093/nar/gku293